Automatic detection and segmentation of indentations and tribological marks by traceable machine vision system

Available online at www.sciencedirect.com

ScienceDirect

Procedia CIRP 138 (2026) 1145–1150

www.elsevier.com/locate/procedia

18th CIRP Conference on Intelligent Computation in Manufacturing Engineering

Automatic detection and segmentation of indentations and tribological marks by traceable machine vision system

Gianfranco Genta[a,*], Giacomo Maculotti[a], Matteo Perrone[a], Maurizio Galetto[a]

[a]*Department of Management and Production Engineering, Politecnico di Torino, C.so Duca degli Abruzzi 24, 10129 Turin, Italy*

* Corresponding author. Tel.: +39-011-090-7257. *E-mail address:* gianfranco.genta@polito.it

Abstract

Automatically segmenting topographical features improves precision of characterization, essential in mechanical characterizations requiring the measurement of residual marks, e.g. Vickers hardness, pin-on-disc. This work demonstrates a method developed within the 22RPT01 BVH-K project which leverages machine vision to segment Vickers indentations and wear tracks on industrially relevant applications, e.g. metals, polymers. The method exploits topographical microscopes, providing traceability, and allows higher precision than operator-based approaches. Isolation of local plasticity effect on feature edge, e.g. pile-up, galling, is also possible, thus providing a strong tool to support primary metrology in improving candidate reference materials and accuracy by correcting edge-effects.

Keywords: Wear; Indentation; Machine vision

1. Introduction

Hardness and tribological tests, both the conventional model ones for testing materials (e.g., pin-on-disc), as well as bench tests for real components, e.g., splines and gears, are essential to investigate the mechanical and wear response of the materials to estimate energy consumption, creation of polluting particulates, and the fatigue life of the components [1–3]. To this end, it is necessary to identify in an accurate and repeatable manner the residual indentation, and the wear through topographical or gravimetric measurements, in terms of the volume of worn material [4]. The identification of the residual indentation is essential for conventional hardness tests, e.g. Brinell and Vickers [5], but accurate determination of the edges is affected by indentation-edge localized plasticity generating phenomena of pile-up, liable of biasing the result [6–8]. Thus, not only it is necessary to accurately measure the indentation extent, but it is also necessary to identify plastically displaced volume of material above the reference surface.

Similarly, the determination of the wear volume, in terms of material removed or plastically displaced, allows for the study of the resistance of different materials and coatings subjected to mechanical contact stresses [9,10]. This is particularly important for the selection and optimization of the materials used in the manufacturing of heavily stressed mechanical components such as gears, bearings, and bushings [11,12]. Moreover, the ability to distinguish between the different wear components is essential depending on the application cases. In fact, the study of materials or components for brake discs, clutch discs, or brake pads focuses on material loss [13,14]. Conversely, the study of plastically displaced material and in general of total damage (removed material and plastically displaced material) is essential in applications with very tight tolerances on shape, e.g., gears and mechanical couplings [15–17]. Measuring the wear volume also allows quantifying the wear rate and the wear coefficient of the material (Archard's equation) which is used in numerical models for the simulation of wear damage [18,19].

10.1016/j.procir.2026.01.197

Therefore, measuring residual indentations and the wear volume is essential, while allowing the distinction between the various components. Today, the most cutting-edge applications prefer, both to address technical limits and for greater simplicity and informativeness, topographical measurements [4,8,20,21]. These, once the measurement is taken, firstly require the identification of the indentation or the wear track, if localized as in the case of pin-on-disc tests [22]. Secondly, they require distinguishing between the different components of plastic deformation and wear, such as the material removed and that displaced or plastically or by redeposition phenomena, and then evaluating their volume [8,23–26]. These components, morphologically, appear, respectively, as valleys of a more or less known shape, continuous and homogeneous (depending on the tribological test considered) and hills at the edge of the valleys themselves. The evaluations of the material volume are mostly carried out through the analysis of the cumulative probability distribution of the measured surface heights h, i.e., the material ratio curve ($M_r(h)$) [27] (also improperly known as Abbot-Firestone $\mathcal{AF}(h)$ curve). The literature [28,29] typically analyses such a curve, and, by identifying a threshold value of heights (h^*), evaluates a pair of topographic parameters: the material volume (Vm) and the void volume (Vv) [27], see Fig. 1. They represent, respectively, the volume of material between the plane described by the threshold h^* and the measured topography, and the volume of missing material between said plane and topography, which respond to the needs of tribological characterization.

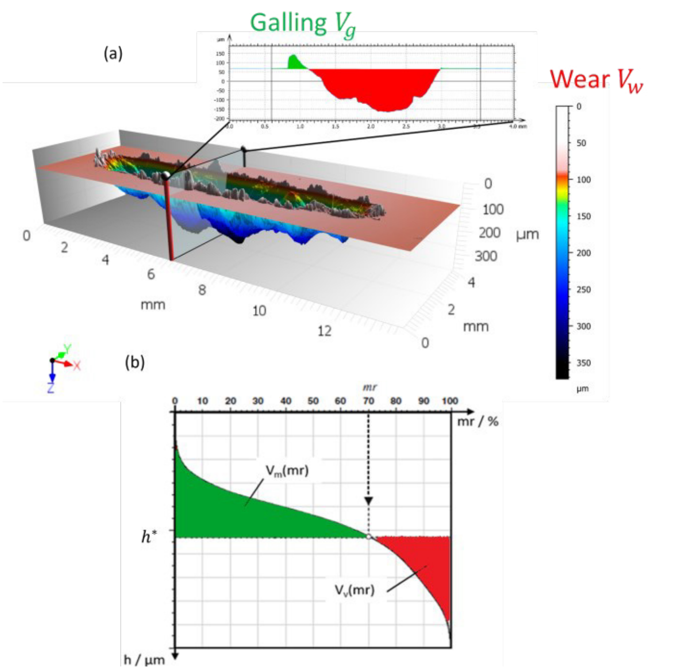

Fig. 1 (a) Example of wear track with removed material (red) and plastically displaced (galling) material (green) and relationship with (b) material ratio curve, indicating relevant surface topography volume parameters.

It is evident that the choice of h^* significantly influences the outcome, and the automation of the selection criterion is essential to guarantee the metrological properties of accuracy and precision necessary for the results of tribological tests and wear analysis. This work in Section 2 will discuss limitations of currently available approaches, and will present an innovative approach aimed at automatically determining such value h^* through a numerical approximation algorithm, in Section 3 will demonstrate the proposed methodology on real case studies of indentations and pin-on-disc wear tracks and, finally, in Section 4 will draw conclusions.

2. Methodology

2.1. Proposed method

Let us consider any surface with topography $Z(x,y)$. This can be modelled as a Gaussian Process (GP) [30,31]:

$$Z(x,y) = S(x,y) + \zeta \quad (1.1)$$

$$\zeta \sim N(\mu, \sigma^2) \quad (1.2),$$

where $S(x,y)$ is the shape, or form, of the topography, and ζ is the stochastic component of the topography, normally distributed with average μ and variance σ^2. The GP model allows thanks to the spatial correlation to include and model in the normally distributed process different length scales, i.e. roughness, texture and waviness. The cumulative distribution function (*cdf*) of the surface heights z is the material ratio curve $M_r(z)$. This can be split in five regions, i.e. peaks, valleys, plateau and transition zones from the formers to the latter.

Let us now suppose to perform any manufacturing process entailing a surface modification, which in particular can be a tribological or hardness test process. This surface modification entails a change of the topography, resulting in a texturing related to the manufacturing signature, e.g. in the case of surface manufacturing or finishing such as machining, grinding, honing [32–35], to the tribological process [20] resulting in wear and plastic displacement, or the residual indentation. If the process is localized and does not alter the surface shape, then, the modification can alter the form while introducing a meso-scale texture, and change the random component of the topography through the different topographical scales, i.e. roughness and waviness, such that:

$$Z_p(x,y) = S(x,y) + S_p(x,y) + \zeta_p \quad (2).$$

If the surface topography is measured both before and after the surface modification, e.g. the tribological process, indentation, and the surfaces are aligned, e.g. by means of machine vision algorithms [20], the difference between the two surfaces can be evaluated as:

$$D = Z_p - Z = S + S_p + \zeta_p - S - \zeta = 0 + S_p + \zeta_2 \quad (3).$$

Thus, the difference has eliminated the original shape leaving a surface topography with the nominal shape of an horizontal plane through 0, surface large scale modifications due to texturing, wear, and plastic displacement (S_p) and a stochastic contribution due to the surface modification normally distributed, i.e. $\zeta_2 = \zeta_p - \zeta$.

For sake of discussion, let us assume that the original surface is flat, such that $S(x,y) = w$, where w is a real constant, i.e. $Z_w(x,y) = w + \zeta$. Let us also remember that for unimodal, as Gamma, normal and t-Student, distributions, the *cdf* is monotonic, S-shaped with one flex point coincident with the mode of the distribution [36]. In particular, for a Normal distribution, as the one of $Z_w \sim N(w + \mu, \sigma^2)$, the flex of the cdf will also be equal to the mean and the median. Therefore, for the considered flat surface, the flex will be at $z^* = w + \mu$. This particular condition is realized by the difference operation, which allows to evaluate $w = 0$. In such a situation, the flex z^* allows to easily distinguish positive and negative features, thus representing the threshold h^*.

However, S_p introduces peaks and valleys, thus severely modifying the shape of the $M_r(z)$, polarizing the tails effect and possibly introducing a strong skewness. Consequently, the difference surface D will be no more normally distributed. In particular, the M_r will present only three relevant portions thanks to the difference operation, i.e. peaks, valleys and a large plateau. The plateau will have a normal distribution due to measurement and registration errors and roughness modifications due to the surface process. However, if the measured surface is significantly larger than the technologically modified surface area, the distribution will be still unimodal, with a M_r with only one flex point.

Accordingly, once registered the surfaces, and evaluated the differences, it is possible to evaluate the flex h^* by means of a numerical approximation, e.g.:

1. Define the mode $\tilde{z}$
2. Define a neighbourhood $I_{\tilde{z}} = \{0.9\tilde{z}, 1.1\tilde{z}\}$
3. Given the inverse relationship $z = M_r^{-1}$, compute the first z' and second z'' derivative by means of numerical weighted partial differences [37]
4. $h^* = \min\{|z''|\}, z \in I_{\tilde{z}}$.

Such numerical procedure allows to avoid severe distortions of the empirical computation of the mode due to the presence of debris and dirt on the surface.

2.2. Advantages with respect to literature approaches

Several approaches have been proposed in the literature to evaluate volume of material of surfaces undergone to tribological processes. Disregarding gravimetric approaches which cannot distinguish components due to galling and wear [4,22], the discussion will be limited to topographical approaches. The first, it is relevant to notice that no work stressed the relevance of measuring the surface both before and after the surface modification. Although this is not always possible and indeed increase the cost of the procedure, working on the modified surface could be a tolerable approximation when dealing with polished surfaces, or whenever the average roughness Sa is significantly smaller than the height range and dispersion of the modified surfaces.

Waterworth [28,38] suggests to fit the central part of the M_r curve by means of a conic equation, i.e. a second order regression. The intersection of the asymptotes of the conic equation identifies the threshold point h^*. Thus, the threshold is not sought as the flex.

Michalski [39,40] suggests to identify the threshold as the flex of the M_r either as the point of the plateau with the maximum curvature, by means of quadratic regressions, or seeking a point with a given slope by means of linear regressions. These methods, however, operates on the M_r, constraining some mathematical properties to the flex point, and not on the derivatives, by means of least-square regressions, which cannot guarantee any property of the derivative [37].

As far as these approaches are concerned, it is worth noticing that they constraint the M_r to a specific trend modelled as piecewise linear or quadratic, considering a large section of the M_r plateau. However, even if the shape of the distribution is known, e.g. normal or Gamma, the *cdf* would be an exponential and the proposed approaches applied higher order regression to non-negligible length portions of the M_r, thus infringing Taylor approximation. Although, the methods have been demonstrated for cylindrical surfaces, they do not have any general applicability. Conversely, the proposed approach, by relying on the registration and difference, allows to inherently remove significant underlying distortions of the distribution, thus approaching a well-known distribution; furthermore, by identifying the flex working on derivatives by means of numerical approaches, it dismisses any additional hypotheses on the distribution of the difference surface. Furthermore, the cumbersome definitions of the approaches and the iterative nature concatenating multiple regression steps would result in an increase of the measurement uncertainty.

Indeed, other works [29] suggests arbitrary thresholding, which have clear lack of generality and are strongly operator dependent. Similarly, other automatic numerical methods [41] define the threshold as a polynomial fit of the surface, highly sensitive to geometric singularities and local features, which are highly likely to be present. Alternatively they segment the surface in several profiles thresholding positive and negative features through the average profile height, which is liable of distorting the results and sensitive to the segmentation direction [4,20].

3. Case Studies

The previous discussion and the literature have shown that operating on the material ratio curve produces significantly more accurate and less uncertain, up to one order of magnitude, results [4,20,22]. Section 2.1 has proposed a methodology to automate and increase the robustness of such approach, while providing proof of the need of evaluating, on a nominally flat surface (which can be in general obtained through the difference method) the threshold to distinguish protruding and recessing features as the flex of the material ratio curve. In the following, the methodology will be tested on some industrially relevant case studies. In particular, it will focus on the capability of segmenting localized features, e.g. pin-on-disc tracks and indentations.

3.1. Experimental set-up

The proposed approach is tested and demonstrated on: plane surfaces undergone tribological tests by linear alternating pin-on-disc (track length of 4 mm) on Aluminium, and circular pin-on-disc (track radius of 5 mm) on PTFE with a load of 5 N, an average speed of 0.05 m/s and a test length of 50 m [4,22]. Both the samples were measured with a Zygo NewView900 coherence scanning interferometer (CSI) with an objective lens Michelson with 5.5× magnification (Numerical Aperture of 0.15 and square Field of View with side of 1.53 mm). Also, a Berkovich micro indentation performed on stainless steel samples with a maximum load of 23 N by means of an Anton

Paar MCT[3] indenter was measured with the same CSI equipped with a Mirau 50× magnification objective (Numerical Aperture of 0.55 and square Field of View with side of 0.17 mm) [8,42].

Measurements were performed in the metrological room of the Mind4Lab at the Department of Management and Production Engineering of the Politecnico di Torino. Analyses are performed coupling an in-house developed MATLAB code implementing the workflow outlined in Section 2.1 with MountainsMap 8.2.

3.2. Results and Discussion

Figures 2 to 4 show the result of the method application to segment localized wear track by pin-on-disc and indentations. As it can be appreciated, the surface resulting from the registration and difference of measurement carried before and after the surface modification phenomenon, presents flat, with no texture and with a negligible roughness, see Fig. 2-4(a). The related material ratio curve is evaluated, and the histogram of the probability density overlaid. As it can be clearly appreciated in Fig. 2-4(b) the probability density, i.e. the histograms, although severely different from the normal distribution ζ, are still unimodal, which guarantees the presence of the flex in the neighbourhood of the mode. The detected threshold allows segmenting the surface as shown in Fig. 2-4(c) and the resulting partitions identify the hills, i.e. protruding features shown in Fig. 2-4(d), and the valleys, i.e. the negative features shown in Fig. 2-4(e).

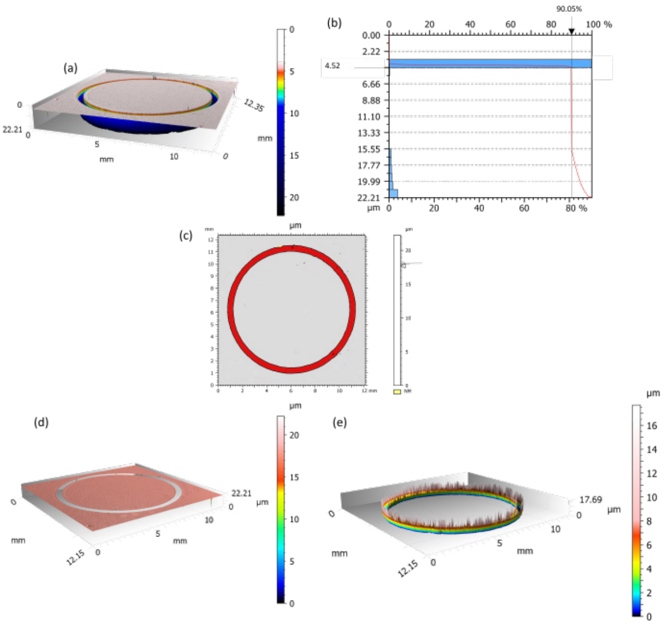

Fig. 2 Circular pin-on-disc on PTFE. (a) Difference surface, (b) material ratio curve with indication of the detected threshold, (c) segmentation based on the evaluated threshold and segmented topography: (d) reference surface, notice the lack of plastically displaced positive features and (e) wear track.

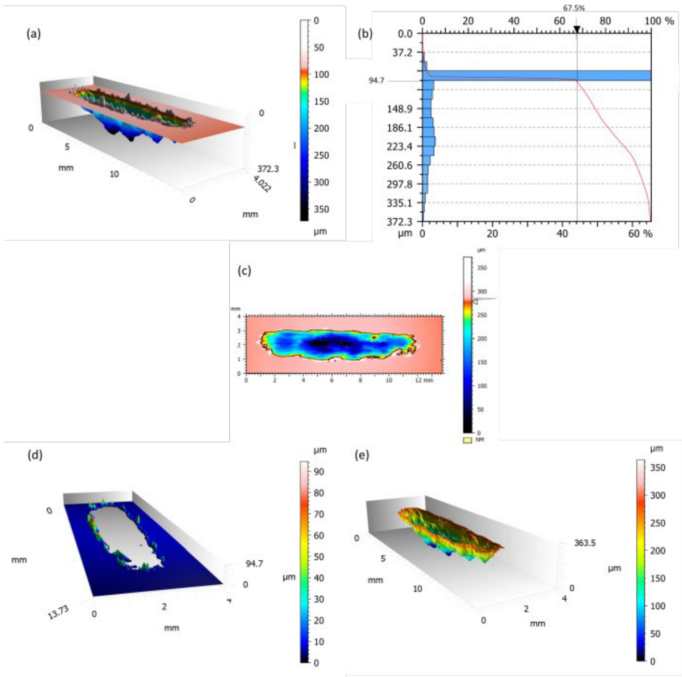

Fig. 3 Linear alternating pin-on-disc on Aluminuim. (a) Difference surface, (b) material ratio curve with indication of the detected threshold, (c) segmentation based on the evaluated threshold and segmented topography: (d) reference surface, with galling, i.e. plastically displaced positive features at the track edge, and (e) wear track.

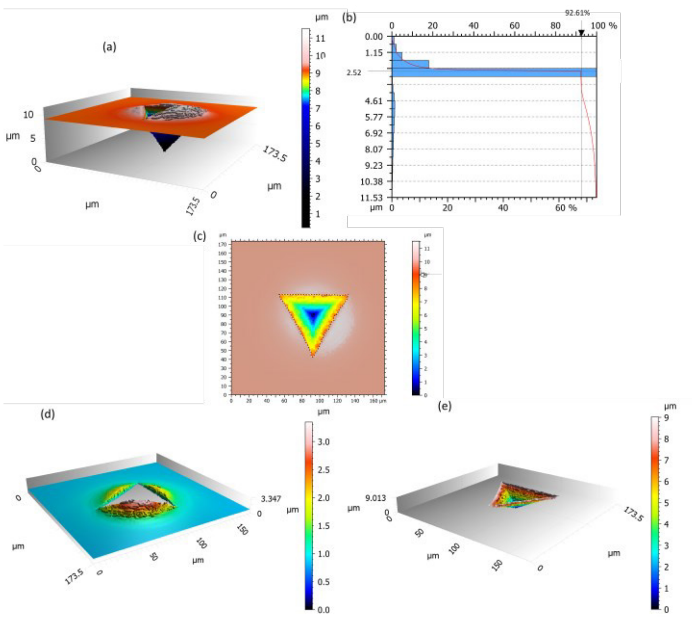

Fig. 4 Berkovich indentation on Stainless Steel. (a) Difference surface, (b) material ratio curve with indication of the detected threshold, (c) segmentation based on the evaluated threshold and segmented topography: (d) reference surface, with pile up, i.e. plastically displaced positive features at the track edge, and (e) residual indentation.

In the case at hand, negative features are related the core surface process resulting in wear (for the pin-on-disc in Fig. 2 and Fig. 3) or plastic deformation (for the indentation in Fig. 4). Depending on the mechanical properties and the grain structure of the material, positive plastic deformations may occur. In the case of wear this is galling, while in the case of indentation it is pile-up. The latter is particularly critical for it biases hardness and Young modulus evaluation obtained from hardness tests. The proposed method, successfully achieved a segmentation of the pile-up material, which could be then exploited to correct bias according to the associated volume or area of contact.

4. Conclusions

This work proposed an algorithm to automatically segment localized wear tracks and indentation. The algorithm allows distinguishing contribution to wear and indentation, separating, removed material and galling, and indentation from pile-up. The algorithm proposed here requires to measure the surface undergone a surface modification process before and after said process, evaluate the difference surface and compute the related material ratio curve. Thanks to its automatic and closed form nature guaranteeing unimodality and searching for the flex of the material ratio curve, compared to other methods currently available, when applied to wear evaluation or pile-up correction it will be able to i) reduce measurement uncertainty, and thus improving precision, ii) ensure accurate measurements, iii) guarantee speed of inspection and measurement, iv) provide an automatic measurement method that v) is not sensitive to arbitrary choices of the operator, and thus robust. Future works will focus on industrial large scale applications of the method to model pile-up and sink-in behaviours of materials during indentation hardness tests.

Acknowledgements

This work has been carried out within the project 22RPT01 TracInd BVK-H which has received funding from the European Partnership on Metrology, cofinanced from the European Union's Horizon Europe Research and Innovation Programme and by the Participating States.

References

[1] Logozzo S, Valigi MC. Wear Assessment and Reduction for Sustainability: Some Applications. In: Quaglia G, Gasparetto A, Petuya V, Carbone G, editors. Proceedings of I4SDG Workshop 2021, Cham: Springer International Publishing; 2022, p. 395–402.
[2] Logozzo S, Valigi M. Green tribology: wear evaluation methods for sustainability purposes. Int J Mechanics Control 2022;23:23–33.
[3] Linke BS. Review on Grinding Tool Wear With Regard to Sustainability. J Manuf Sci Eng 2015;137.
[4] Maculotti G, Goti E, Genta G, Mazza L, Galetto M. Uncertainty-based comparison of conventional and surface topography-based methods for wear volume evaluation in pin-on-disc tribological test. Tribol Int 2022;165:107260.
[5] Tabor D. The hardness of metals. London, UK: Oxford University Press; 1951.
[6] Cheng YT, Cheng CM. Effects of 'sinking in' and 'piling up' on estimating the contact area under load in indentation. Philos Mag Lett 1998;78:115–20.
[7] Galetto M, Kholkhujaev J, Maculotti G. Improvement of instrumented indentation test accuracy by data augmentation with electrical contact resistance. CIRP Ann – Manuf Technol 2023;72:469–72.
[8] Kholkhujaev J, Maculotti G, Genta G, Galetto M. Metrological Comparison of Available Methods to Correct Edge-Effect Local Plasticity in Instrumented Indentation Test. Materials 2023;16:4262.
[9] Lucchetta G, Giusti R, Vezzù S, Bariani PF. Investigation and characterization of Stellite-based wear-resistant coatings applied to steel moulds by cold-spray. CIRP Ann Manuf Technol 2015;64:535–8.
[10] Kowandy C, Richard C, Chen YM. Characterization of wear particles for comprehension of wear mechanisms. Wear 2008;265:1714–9.
[11] Gu P, Zhu C, Mura A, Maculotti G, Goti E. Grinding performance and theoretical analysis for a high volume fraction SiCp/Al composite. J Manuf Process 2022;76:796–811.
[12] Maculotti G, Goti E, Genta G, Mazza L, Galetto M. Comprehensive mechanical and tribological characterization of metal-polymer PTFE+Pb/Bronze coating by in-situ electrical contact resistance measurement augmented tribo-mechanical tests. Tribol Int 2024;193:109397.
[13] Chandra Verma P, Menapace L, Bonfanti A, Ciudin R, Gialanella S, Straffelini G. Braking pad-disc system: Wear mechanisms and formation of wear fragments. Wear 2015;322–323:251–8.
[14] Ostermeyer GP. Friction and wear of brake systems. Forsch Ingenieurwes 2001;66:267–72.
[15] Goti E, Mazza L, Manuello Bertetto A. Wear tests on PTFE+pb linings for linear pneumatic actuator guide bushings. International Journal of Mechanics and Control 2020;21:155 – 162.
[16] Goch G, Guenther A, Peng Y, Ni K. Gear metrology – An update. CIRP Ann Manuf Technol 2023;72:725–51.
[17] Wright NA, Kukureka SN. Wear testing and measurement techniques for polymer composite gears. Wear 2001;251:1567–78.
[18] Rabinowicz E. Friction and Wear of Materials. 2nd Editio. New York: John Wiley & Sons; 1995.
[19] Bayer RG. Mechanical Wear Fundamental and Testing. New York, NY, USA: Marcel Dekker Inc.; 2004.
[20] Genta G, Maculotti G. Uncertainty evaluation of small wear measurements on complex technological surfaces by machine vision-aided topographical methods. CIRP Ann Manuf Technol 2021;70:451-454.
[21] Takimoto RY, de Sales Guerra Tsuzuki M, Ueda EK, Sato AK, de Castro Martins T, Cousseau T, Tanaka D, Sinatora A. Rough Surface Wear Analysis Using Image Processing Techniques. IFAC-PapersOnLine 2016;49:7–12.
[22] Maculotti G, Goti E, Genta G, Marchiandi G, Mura A, Mazza L, Galetto M. Effect of track geometry on the measurement uncertainty of wear in pin-on-disc tribological test. Proceedings of the 21st International Conference and Exhibition of EUSPEN 2021.
[23] ISO 18535-2:2016 Diamond-like carbon films - Determination of friction and wear characteristics of Diamond-like carbon films by ball-on-disc method. ISO, Genève
[24] ASTM G40-17 Standard Terminology Relating to Wear and Erosion. ASTM International, West Conshohocken, PA (USA).
[25] ASTM G99-17 Standard Test Method for Wear Testing with a Pin-on-Disk Apparatus. ASTM International, West Conshohocken, PA (USA).
[26] ASTM G133-95 Standard Test Method for Linearly Reciprocating Ball-on-Flat Sliding Wear. ASTM International, West Conshohocken, PA (USA).
[27] ISO 25178-2:2021 Geometrical product specifications (GPS) — Surface texture. Areal Part 2: Terms, definitions and surface texture parameters. ISO, Genève.
[28] Waterworth A. Quantitative characterisation of surface finishes on stainless steel sheet using 3D surface topography analysis. PhD Thesis. University of Huddersfield, 2006.
[29] Pawlus P, Reizer R, Wieczorowski M, Krolczyk G. Material ratio curve as information on the state of surface topography—A review. Precis Eng 2020;65:240–58.
[30] Maculotti G, Genta G, Quagliotti D, Galetto M, Hansen HN. Gaussian process regression-based detection and correction of disturbances in surface topography measurements. Qual Reliab Eng Int 2022; 38:1501–1518.
[31] Maculotti G, Genta G, Quagliotti D, Hansen HN, Galetto M. Comparison of methods for management of measurement errors in surface topography measurements. Proc CIRP 2023; 118:1084–1089.
[32] Brown CA, Hansen HN, Jiang XJ, Blateyron F, Berglund J, Senin N, et al. Multiscale analyses and characterizations of surface topographies. CIRP Annals 2018;67:839–62. https://doi.org/10.1016/j.cirp.2018.06.001.

[33] Bruzzone AAG, Costa HL, Lonardo PM, Lucca DA. Advances in engineered surfaces for functional performance. CIRP Ann Manuf Technol 2008;57:750–69.
[34] Jiang XJ, Whitehouse DJ. Technological shifts in surface metrology. CIRP Ann Manuf Technol 2012;61:815–36.
[35] Whitehouse DJ. Typology of Manufactured Surfaces. Annals of the CIRP 1971;19:417–31.
[36] Johnson NL, Kotz S. Distributions in statistics. Continuous univariate distributions. 1. Houghton Mifflin Co.; 1970.
[37] Maculotti G, Genta G, Lorusso M, Pavese M, Ugues D, Galetto M. Instrumented Indentation Test: Contact Stiffness Evaluation in the Nano-range. Nanomanufacturing and Metrology 2018;2:16–25.
[38] Leach R. Characterization of Areal Surface Texture. 2013. Springer, Berlin
[39] Michalski J, Pawlus P. Characterization of the shape of the roughness profile ordinate distribution of honed cylinder surfaces. Wear 1993;161:135–43.
[40] Michalski J, Pawlus P. Description of the bearing length curve of the inner surface of piston engine cylinders. Wear 1992;157:207–14.
[41] Mountains Map. www.digitalsurf.com.
[42] Kholkhujaev J, Maculotti G, Genta G, Galetto M. Calibration of machine platform nonlinearity in Instrumented Indentation Test in the macro range. Precis Eng 2023;81:145–57.